

Learning Path Constraints for UAV Autonomous Navigation under Uncertain GNSS Availability

paper #4985

Abstract

This paper addresses a safe path planning problem for UAV urban navigation, under uncertain GNSS availability. The problem can be modeled as a POMDP and solved with sampling-based algorithms. However, such a complex domain suffers from high computational cost and achieves poor results under real-time constraints. Recent research seeks to integrate offline learning in order to efficiently guide online planning. Inspired by the state-of-the-art CAMP (Context-specific Abstract Markov decision Process) formalization, this paper proposes an offline process which learns the path constraint to impose for online POMDP solving. More precisely, the offline learnt constraint selector returns the best path constraint according to the GNSS availability in the environment. This constraint is then imposed during online planning to reduce the policy search space. Conclusions of experiments, carried out for different environments, show that using the proposed approach allows to improve the quality of a solution reached by an online planner, within a fixed decision-making timeframe, particularly when GNSS availability probability is low.

Introduction

Solving autonomous navigation problems consists in finding a path from an initial position to a goal with a maximum efficiency, while avoiding the obstacles. These problems become challenging when the vehicle state is uncertain. Particularly, most of Unmanned Aerial Vehicles (UAVs) are equipped with a Global Navigation Satellite System (GNSS) receiver as navigation system. In an urban environment, the visibility of the GNSS satellite constellation can be reduced by the buildings surrounding the UAV, the precision or even the availability of the GNSS position estimate can then be significantly altered, what can lead to a fatal collision.

(Delamer, Watanabe, and Ponzoni Carvalho Chanel 2021) formalize the UAV urban navigation problem under uncertain GNSS availability as a Partially Observable Markov Decision Process (POMDP) (Kaelbling, Littman, and Cassandra 1998). The latter is a principled approach to solve planning problems under uncertainty. However, POMDP planning faces two notorious problems. The first one is the *curse of dimensionality*: the size of the belief state space grows up

exponentially with that of the state space. The second problem is the *curse of history*: the number of action/observation sequences to evaluate during research grows up exponentially with the planning horizon (Pineau, Gordon, and Thrun 2006). The use of a Partially Observable Monte-Carlo Planning (POMCP) (Silver and Veness 2010) algorithm makes it possible to overcome these difficulties. Nevertheless, the performance remains dependent on the search depth reached within the planning horizon, which is itself dependent on the *branching factor* of the search tree (Hostetler, Fern, and Dietterich 2014). The branching factor includes both the *action factor*, *i.e.* the number of actions available in each belief state, and the *stochastic factor*, *i.e.* the number of possible observations for each action. The stake is then to reduce the branching factor in order to scale up planning. This is all the more important for online planning: the planner has to make a decision quickly whereas the long-planning horizon of such a real-world task incurs prohibitive computational cost. For that, incorporating domain abstraction is a promising approach. (Chitnis et al. 2021) introduce Context-specific Abstract Markov Decision Process (CAMP), an abstraction of the original MDP model, obtained by imposing the *best constraint* on the states and actions considered by the agent. This best constraint is chosen by an offline learnt *context selector* according to the *features* of a task.

Inspired by this CAMP domain abstraction, this paper proposes to learn offline the context selector and to impose the best constraint returned in order to reduce the policy search space during online POMDP solving, for the UAV urban navigation problem. The context selector returns the constraint which reduces the UAV position state space while preserving the solution optimality, in function of the GNSS availability probability map of a task. Unlike the original CAMP, we address a partially observable domain. As states are not fully observable, applying action space abstraction is not straightforward. Nevertheless, a state space abstraction can be achieved through modification of the cost function for penalizing the constraint violation, which will modify the action outcomes. Moreover, contrary to the model proposed in the CAMP paper, the states and actions are not factored. Hence, imposing a constraint does not render some variables irrelevant, which could then have been dropped. Additionally, as our objective is to perform online planning for the UAV safe navigation problem, whereas an offline

POMCP variant is used in the offline process, an online version is applied for planning. As a result, we investigate the use of different algorithms for learning and planning, which has not been done in the original work of CAMP. Thus, regarding the UAV navigation problem with uncertain GNSS availability, our contribution is twofold: (i) we investigate if domain abstraction, by adapting the CAMP framework for a partially observable domain, gives better results when compared to a full POMDP model, and (ii) we evaluate if such a CAMP-inspired approach is robust if we use a different algorithm for learning and planning.

After providing the theoretical background and the related work in the next section, we present the CAMP method adapted to our problem in Section 3. Experimental results are reported in Section 4, demonstrating the planning performance improvement. Finally, Section 5 includes concluding remarks and future works.

Background and Related Work

POMDP Preliminaries

A POMDP (Kaelbling, Littman, and Cassandra 1998) is defined as a tuple $(\mathcal{S}, \mathcal{A}, \Omega, \mathcal{T}, \mathcal{O}, \mathcal{C}, b_0, \gamma)$, where \mathcal{S} , \mathcal{A} , and Ω denote respectively spaces of states, actions, and observations. The *transition function* $\mathcal{T}(s, a, s') = p(s'|s, a)$ represents the dynamics of the agent as the probability of transitioning from s to s' by taking action a . The *observation function* $\mathcal{O}(a, s', o) = p(o|s', a)$ specifies the probability of observing o after taking action a to reach s' . The *cost function* $\mathcal{C}(s, a)$ defines the cost of taking action a in s . b_0 denotes the initial belief state. $\gamma \in [0, 1]$ is a discount factor expressing a preference for minimizing immediate over future cost.

POMDPs capture partial observability of the system using the *belief state* b , i.e. a probability distribution over \mathcal{S} , that is updated after each action a and observation o using the Bayes' rule. A POMDP policy $\pi : \mathcal{B} \rightarrow \mathcal{A}$ prescribes an action for each belief state in the belief space \mathcal{B} . Solving a POMDP requires finding the *optimal policy* π^* minimizing the expected future cost, called the *value*, for all $b \in \mathcal{B}$. The value of the policy π^* in belief b is defined as:

$$V^{\pi^*}(b) = \min_{\pi} \mathbb{E} \left[\sum_{t=0}^{\infty} \gamma^t \mathcal{C}(b_t, \pi(b_t)) \mid b_0 = b \right] \quad (1)$$

Additionally, the Q -value of action a in belief b can be defined as:

$$Q^{\pi}(b, a) = \mathbb{E} \left[\mathcal{C}(b, a) + \sum_{t=1}^{\infty} \gamma^t \mathcal{C}(b_t, \pi(b_t)) \right] \quad (2)$$

UAV Urban Navigation POMDP-based Problem

The original planning model, proposed by (Delamer, Watanabe, and Ponzoni Carvalho Chanel 2021), is formalized as a Mixed-Observability Markov Decision Process (MOMDP) (Ong et al. 2010), a special class of the POMDP framework. The state space is factorized into fully, s_v , and partially, s_h , observable state variables, what reduces the belief state space dimension, and in turn, reduces policy computation time. The state tuple $s = (s_h, s_v) \in \mathcal{S}$ is defined with

$s_h = (\mathcal{X}, \mathcal{V}, \beta_a)$ where \mathcal{X} and \mathcal{V} are the vehicle position and velocity, and β_a is the IMU acceleration measurement bias, and $s_v = (F_{col}, F_{GNSS}, P, t_{flight})$ with F_{col} and F_{GNSS} the collision and GNSS availability Boolean flags, P the estimation error covariance matrix over s_h , and t_{flight} the flight time elapsed. An action $a \in \mathcal{A}$ corresponds to the desired velocity direction. The action space \mathcal{A} is a finite set of 10 actions, following 8 radial directions in the 2D horizontal plane, plus up and down. An observation $o \in \Omega$ is defined as the sub-tuple $o = s_v$ of the state tuple, given a full observability of (F_{col}, F_{GNSS}) and a deterministic transition of (P, t_{flight}) . As s_v depends on s_h , the observation $o = s_v$ will modify the distribution of s_h . In consequence, the complete state s remains partially observable. This partial state observability limits the branching factor of the search tree. The transition function follows a GNC (Guidance, Navigation and Control) model, composed of the vehicle motion model, a guidance law, a state estimator, and the IMU and GNSS sensor models. The GNSS availability F_{GNSS} affects the error covariance P , which affects the belief state b' after transition. In brief, P grows when GNSS is unavailable, resulting in more collision risk. Finally, the cost function is defined as:

$$\mathcal{C}(s, a) = \begin{cases} 0 & \text{if goal reached} \\ K_{col} - t_{flight} & \text{if collision} \\ \Delta T_a & \text{otherwise} \end{cases} \quad (3)$$

with $\Delta T_a > 0$ the action execution time, and $K_{col} > 0$ the cost penalty in case of collision. When a collision occurs, the cost is this penalty subtracted with the flight time elapsed. Added to the sum of the previous action execution times, all the collision paths are then equally penalized.

MinPOMCP-GO Algorithm

(Delamer, Watanabe, and Ponzoni Carvalho Chanel 2021) propose the POMCP - Goal-Oriented (POMCP-GO) algorithm, an offline goal-oriented variant of POMCP (Silver and Veness 2010). It samples a state s from the initial belief state b_0 corresponding to the *root node*, and simulates action/observation sequences, through *trials*, in order to evaluate actions while building a tree of nodes. To perform a trial, POMCP-GO follows a given action selection strategy and a heuristic node value initialization. For the action selection, it relies on the Upper Confidence Bounds (UCB1) strategy (Kocsis and Szepesvári 2006) to deal with the exploration-exploitation dilemma. A trial is stopped when a terminal state is reached (a goal or a collision state), and this procedure is repeated during a fixed timeframe.

Each tree node h represents a history of action/observation sequences from the initial belief state. The Q -value (Eq. 2) of a belief state is approximated by $Q(h, a)$, which is the mean cost returned from all trials started from h when action a was selected. This approximation incurs a well-known bias, which decreases as the number of trials increases (Keller and Helmert 2013). To accelerate the policy value convergence by reducing the Q -value bias, (Carmo et al. 2020) propose the MinPOMCP-GO algorithm which uses a *Min-Monte-Carlo backup* (Keller and Helmert 2013).

The present paper approach is based on this algorithm. During tree building, MinPOMCP-GO initializes the Q -value of a newly created node to a pre-computed heuristic value, corresponding to the flight time left to the goal estimated by the Dijkstra algorithm (Dijkstra 1959). Even if this heuristic function is more informative than the traditional rollout used in POMCP, it does not consider GNSS availability probability. This is only indirectly considered, by back-propagating the cost penalty when a collision occurs, hence sampling trajectories that may lead to collisions due to the uncertain UAV position estimate.

Domain Abstraction

Sampling-based algorithms, such as POMCP and variants, suffer from exponential complexity with respect to the branching factor of the search tree. In our UAV navigation problem under uncertain GNSS availability, the solver cannot explore enough, within a short decision-making time-frame, to prevent collisions. In difficult environments, with obstacles reducing GNSS availability probability, navigation mission safety may be compromised. So, we focus on incorporating domain abstraction to reduce the branching factor and thus to improve online planning solutions.

State Aggregation. One well-known technique of domain abstraction is *state aggregation*: the state space is reduced by clustering equivalent states, *i.e.* states that share some fully-identical properties - *exact aggregation* - or nearly-identical properties - *approximate aggregation* - and treating each of these resulting state clusters as one. In (Li, Walsh, and Littman 2006), the authors list the existing methods of exact state aggregation and unify them to deduce five generic functions. However, since two states rarely share some fully-identical properties, exact abstraction is often useless, while approximate abstraction can achieve greater degrees of compression. In (Abel, Hershkowitz, and Littman 2016), the authors present four types of approximate aggregation and demonstrate that they lead to a bounded loss of optimality of behavior. In (Hostetler, Fern, and Dieterich 2014), the authors generalize the formulation of two of these four types of aggregation and apply them to Monte-Carlo Tree Search (MCTS). AS-UCT (Jiang, Singh, and Lewis 2014), ASAP-UCT (Anand et al. 2015), and OGA-UCT (Anand et al. 2016) are other implementations of state or state-action pair aggregation to UCT, a MCTS algorithm variant. All of these methods have not been applied in the partially observable framework.

Hierarchical Planning. Another approach to domain abstraction is *hierarchical planning*. It consists in decomposing the planning problem into a network of independent sub-goals. *Hierarchical Dynamic Programming* (HDP) (Bakker, Zivkovic, and Kröse 2005) is an example of hierarchical planning for navigation problems. A hierarchy of MDPs is constructed and solved using a hierarchical variation of value iteration. *Abstract Markov Decision Process* (AMDP) (Gopalan et al. 2017) is a more general method, which allows any MDP planner to be used. Both HDP and AMDP are *top-down* approaches: they select the subgoal before

performing planning to reach it. Contrary to *bottom-up* approaches, they present the advantage that planning is necessary only for subgoals used for task completion. Nevertheless, the way to define appropriate subgoals remains an open question.

Integrating Learning for Planning. A third method is to integrate an offline learning phase as a first step, to guide the search during online planning. The CAMP approach (Chitnis et al. 2021), that has inspired this paper, is part of this category. It searches the best reduced state and action spaces by imposing a constraint learnt according to the features of a task. Another example is Macro-Action Generator-Critic (MAGIC) (Lee, Cai, and Hsu 2021), a kind of *temporal abstraction*, which learns the more efficient set of candidate macro-actions to cut down the effective planning horizon.

As previously discussed in the MinPOMCP-GO Algorithm Section, GNSS availability probability is only considered by back-propagating the collision cost. The planning efficiency can hence be improved by using this information to further focus the search on more relevant areas, *i.e.* where GNSS is more likely available. For this purpose, the CAMP method seems a good candidate to leverage. Implementing a similar approach for our problem allows to reduce the UAV position state space in function of a probability map of GNSS availability, considering this as a task feature.

Learning Path Constraints based on GNSS Availability

Approach Overview

The objective of the CAMP method (Chitnis et al. 2021) is to learn a context selector $f : \Theta \rightarrow \mathcal{C}$. Each *training task* corresponds to a *feature vector* $\theta \in \Theta$. For each feature vector, the best constraint $C^* \in \mathcal{C}$ is identified. The pairs (θ_i, C_i^*) are given to a neural network to learn f . Once the context selector f is learnt, the best constraint C^* returned from the feature vector θ is then imposed to guide online planning.

In our navigation problem under uncertain GNSS availability, we assume a given environment, *i.e.* known obstacles on a map, and a given navigation mission, *i.e.* fixed initial position and goal. Figure 1 describes our application of the context selector learning process to our problem. The probability maps of GNSS availability are used as feature vectors. For each training map of GNSS availability probability, the best constraint is identified. We define a constraint as a corridor of the environment in which the UAV must stay, that we evaluate by performing planning within a *training timeout*. Then, these probability maps of GNSS availability and the associated best constraints are used to train the context selector. Finally, the *test tasks* are solved online, imposing the best constraints returned by the context selector from the test maps of GNSS availability probability. Each step of this process is detailed in the following sub-sections.

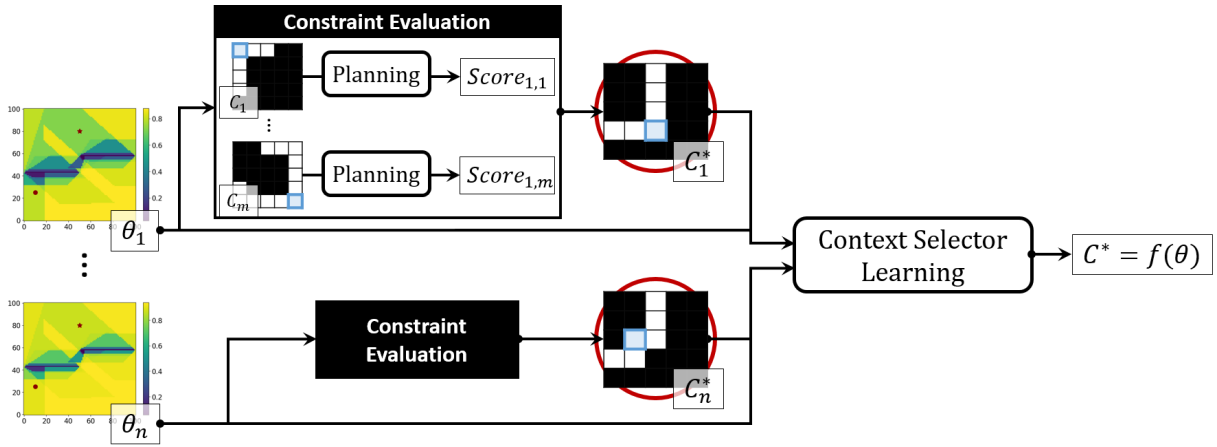


Figure 1: Learning the context selector f by identifying the best constraint C_i^* , for each training task i associated to a probability map of GNSS availability θ_i .

Feature Vectors

As previously discussed, the GNSS availability is crucial to determine safe paths for our UAV. As the GNSS satellites are orbiting around the Earth, the GNSS availability probability varies with the time-of-the-day even for a fixed obstacle environment. We then propose to compute navigation constraints based on probability maps of GNSS availability to reduce the UAV position state space.

A quality of the GNSS position estimate is given as a metric called *Position Dilution Of Precision* (PDOP) (Kleijer, Odijk, and Verbree 2009). Given satellite geometry and user location, a PDOP map is generated by using a GNSS simulator. We consider PDOP value as a standard deviation of the GNSS positioning error, assumed to follow a zero-mean Gaussian distribution (Delamer, Watanabe, and Ponzoni Carvalho Chanel 2021). Then, the PDOP map is transformed to a probability map of GNSS availability by using erf , the Gauss error function, and by setting a maximum position error threshold ϵ :

$$\Pr(F_{GNSS} = 1) = \text{erf} \left(\frac{\epsilon}{\sqrt{2}\text{PDOP}} \right). \quad (4)$$

First, we generated the test task features by setting different ϵ values, to cover the easy and difficult cases where GNSS is most-like available/unavailable. Then, the training task features were generated by linear combination of these test task features with randomly selected coefficients, for more feature variety.

Constraint Definition and Evaluation

Constraint Definition. We divide the environment map into $n_L \times n_l \times n_h$ areas in a uniform way. n_L denotes the number of areas over the length, n_l over the width, and n_h over the height. For each of these areas, we define a corridor of areas leading from the initial position to the goal one, passing through this area, called *passage area*. For that, we concatenate the paths resulting from the A* algorithm (Hart, Nilsson, and Raphael 1968) from the area including the initial position to this passage area, and from the latter to the area including the goal position. We use the number of areas

constituting the path as cost function in the A* algorithm. We obtain thus at most $n_L \times n_l \times n_h$ different corridors of areas, corresponding to *candidate constraints*, in which the UAV is allowed to navigate. The sub-figure in the middle of Figure 2 shows a candidate constraint defined by dividing the environment map into $(n_L = 5) \times (n_l = 5) \times (n_h = 1)$ areas, and using the top left area as passage area, which is highlighted in blue.

Planning with Constraint. For each training map of GNSS availability probability, all the candidate constraints are evaluated. For that, planning imposing the candidate constraint is performed. We use the MinPOMCP-GO planning algorithm (Carmo et al. 2020), adapting the heuristic function, which estimates the flight time left to the goal, so that the constraint is respected. Figure 2 illustrates an example of the heuristic map obtained from a given environment, navigation mission, and candidate constraint. On the environment map on the left, as on the following maps, the initial position and the goal are respectively represented by a point and a star, and the obstacles are depicted in yellow. On the heuristic map on the right, the estimated flight time left to the goal is represented inside the constraint.

To impose a constraint, the cost function of the planning model (Eq. 3) is also adapted so that it considers a violation of the constraint as a terminal state which leads to a cost penalty K_{constr} . In addition, the collision cost is saturated by a minimal threshold $K_{col_{thr}}$, as some imposed constraints incur long flight times. The cost function then becomes:

$$\mathcal{C}(s, a) = \begin{cases} 0 & \text{if goal reached} \\ \max(K_{col} - t_{flight}, K_{col_{thr}}) & \text{if collision} \\ K_{constr} & \text{if constraint violation} \\ \Delta T_a & \text{otherwise} \end{cases} \quad (5)$$

Best Constraint Identification. In the original CAMP approach (Chitnis et al. 2021), a candidate constraint is evaluated using a score formulation, which expresses the trade-off between *how much planning is sped up* and *how much optimality is preserved* imposing this constraint. The planning

time and the policy value are obtained as means over several online-solved episodes. In our method, we perform offline planning to evaluate the candidate constraints. Hence, reaching the convergence on the policy value is required to estimate the planning time and the policy value. However, this convergence is difficult to judge and achieve it can take too long. Therefore, to evaluate a candidate constraint, we stop planning when a *training timeout* is reached, and we express the score as the inverse of the resulting initial belief state value $V^\pi(b_0)$. For a probability map of GNSS availability θ_i , the candidate constraint that achieves the highest score, *i.e.* the lowest initial belief state value, is chosen as the best constraint, and is noted C_i^* .

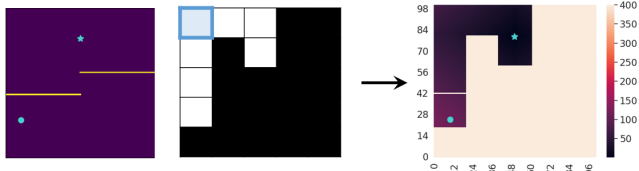


Figure 2: Generation of the heuristic map (right) from an environment, a navigation mission (left), and a candidate constraint (middle).

Context Selector Learning and Online Planning

The training maps of GNSS availability probability $\{\theta_i\}$ and the associated best constraints $\{C_i^*\}$ are used to train a neural network with cross-entropy loss, resulting in the context selector f (Fig. 1). The generic neural network available in the CAMP framework is applied, with the proposed Fully Connected Network architecture (Chitnis et al. 2021).

At test time, the best constraint is returned by the context selector, given the probability map of GNSS availability of the test task: $C^* = f(\theta)$. This constraint is then integrated in the model for online planning to reduce the UAV position state space, by imposing to compute navigation paths that stay within the constraint. We use two planning algorithms to compute these navigation paths. The first one is MinPOMCP-GO, also used for evaluating the candidate constraints in the training phase. The second algorithm is MinPOMCP-GO*: it is a variant of MinPOMCP-GO in which trials end whenever a previously unvisited leaf node is encountered, instead of ending a trial only when a terminal state is reached. MinPOMCP-GO* is aimed to be used online, as it produces more trials with a shortest depth, hence favoring short-term performance that would help avoiding collisions, while taking into account actual observations in an online setting.

Experiments

We implement the previously described method to three navigation benchmark environments available in (Mettler et al. 2010): *Cube Baffle*, containing two cubes, *Wall Baffle*, containing two walls, and the real downtown of *San Diego*. They are illustrated in Figure 3.

To evaluate our approach, four test tasks are solved for each environment, numbered from 1 to 4, corresponding to the maps presenting from the lowest to the highest GNSS

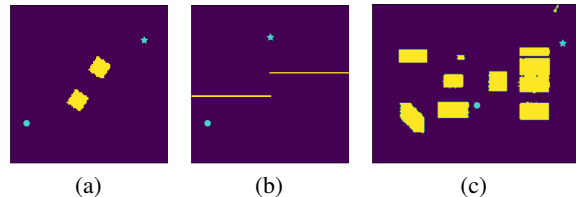


Figure 3: *Cube Baffle* (a), *Wall Baffle* (b), and *San Diego* (c).

availability probabilities. We compare the results obtained imposing the best constraint returned by the context selector with those obtained without constraint. The performance metrics are the number of collisions and the mean costs obtained considering a fixed decision-making timeframe. The lower they are, the better performance is.

Material

To carry out the experiments, we use a supercomputer constituted of 24 cores. For each of these cores, the frequency is of 2.60 GHz, the Random Access Memory size is of 96 Gb, and the cache size is of 19.25 Mb.

Settings

In the following, we describe the settings used in our experiments. The GNC model and the reference velocity settings are the same as those described in (Delamer, Watanabe, and Ponzoni Carvalho Chanel 2021).

Initial Position and Goal. The mean initial position is set to $X_0 = [10, 25, 5]$ for *Cube Baffle* and *Wall Baffle*, and $X_0 = [110, 60, 5]$ for *San Diego*. The goal position is set to $X_G = [85, 78, 5]$ for *Cube Baffle*, $X_G = [50, 80, 5]$ for *Wall Baffle*, and $X_G = [200, 125, 5]$ for *San Diego*.

Map Decomposition. The map size of *Cube Baffle* and *Wall Baffle* is $[101, 101, 21]$. For *San Diego*, it is $[217, 167, 24]$. The maps are uniformly divided into $(n_L = 5) \times (n_t = 5) \times (n_h = 1)$ areas.

Model and Solver. The factor γ is set to 1 and the action cost ΔT_a is set to 2.2. The collision penalty K_{col} , its threshold $K_{col_{thr}}$, and the constraint violation penalty K_{constr} (Eq. 5) are respectively set to 450, 350, and 450. The exploration coefficient c of UCB1 is set to 6.

Training Tasks. The training timeout is set to 2 minutes and the number of training tasks, *i.e.* the number of probability maps of GNSS availability used for training, is 30.

Neural Network and Test Tasks. The neural network loss threshold is set to 1.8. The decision-making timeframe is set to 2 seconds and the number of test tasks, *i.e.* the number of probability maps of GNSS availability used for testing, is 4. These maps are generated with the error thresholds: $\epsilon = 1, 2, 5, \text{ and } 10$ meters. For each test task, 50 episodes are launched.

Results

The performance metric values obtained for each environment are summarized in Table 1. The probability maps of GNSS availability at the initial and goal altitude are displayed as background of the following figures, the resulting

paths are plotted in red and the collisions are represented by black dots.

For the *Cube Baffle* environment, the costs obtained without constraint and imposing the best constraint, using MinPOMCP-GO or MinPOMCP-GO*, are similar for all the test tasks. Indeed, the UAV does not fly close enough to the cubes and the GNSS availability probability is sufficiently high. Hence, very few collisions occur, even without constraint. Figure 4 shows the resulting paths without constraint and imposing the best constraint for the first test task, corresponding to the lowest GNSS availability probabilities. The imposed constraint makes the resulting paths deviate to avoid the zones of possible GNSS loss to reduce the collision risk.

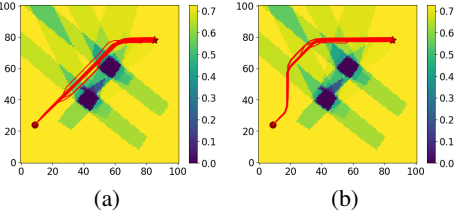


Figure 4: Results obtained for *Cube Baffle*, for test task (1): paths obtained using MinPOMCP-GO*, without constraint (a), and with the best constraint (b).

For the *Wall Baffle* environment, with MinPOMCP-GO or MinPOMCP-GO*, the number of collisions and the cost obtained imposing the best constraint are considerably lower than those without constraint for the test tasks (1) and (2), corresponding to the two maps presenting the lowest GNSS availability probabilities. For test task (1), using MinPOMCP-GO, the number of collisions obtained imposing the best constraint is reduced of almost 72%; and using MinPOMCP-GO*, it is reduced to 0. Figure 5 shows the resulting paths without constraint and imposing the best constraint. For these first two test tasks, the best constraint forces to fly over the wall, where GNSS availability probability is greater, instead of flying between the two walls as obtained when no constraint is imposed. Even if the flight time becomes a bit longer, the cost is much reduced because less collisions occur. That is, the mission safety is largely improved. For the third test task, with MinPOMCP-GO or MinPOMCP-GO*, the cost is slightly increased when imposing the best constraint, still favoring the safer paths flying over the wall. Finally, for the fourth test task, presenting the highest GNSS availability probabilities, the best constraint only imposes to slightly move away from the first wall. It results in a slight decrease of the collision rate, with MinPOMCP-GO or MinPOMCP-GO*.

The *San Diego* environment includes multiple buildings, that incurs a lot of regions where GNSS availability probability is low. Without constraint, the mission leads to a collision in most episodes, for each test task. The best constraints returned correspond to pass to the left of the obstacles (Fig. 6). With MinPOMCP-GO or MinPOMCP-GO*, the number of collisions and the cost are decreased imposing the best constraint, particularly for the two maps presenting the highest GNSS availability probabilities, test tasks (3) and (4). For the third test task, the cost is decreased to almost 46% using

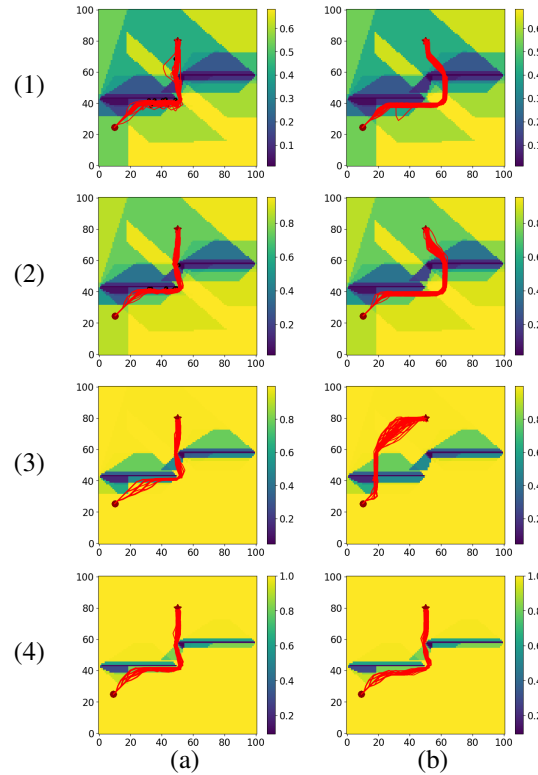


Figure 5: Results obtained for *Wall Baffle*: paths obtained using MinPOMCP-GO*, without constraint (a), and with the best constraint (b)

MinPOMCP-GO*, and for the fourth task, it is reduced to almost 38% using MinPOMCP-GO.

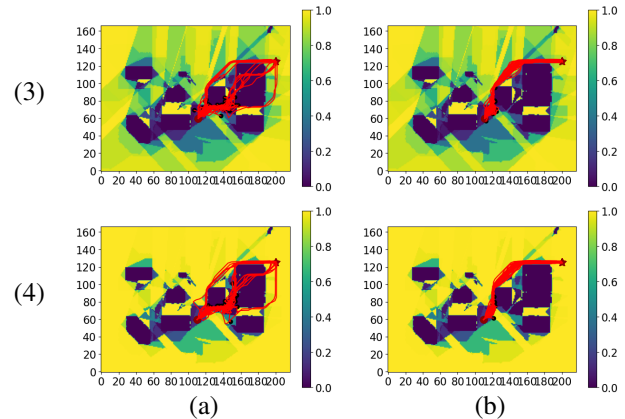


Figure 6: Results obtained for *San Diego*, for test tasks (3) and (4): paths obtained using MinPOMCP-GO*, without constraint (a), and with the best constraint (b)

In conclusion, for the three environments, imposing the best constraint always reduces the number of collisions, with any MinPOMCP-GO variant. This gain on the number of collisions and the one on the cost are much greater for difficult environments, comprising multiple obstacles and presenting low GNSS availability probabilities. Moreover, although the context selector is learnt from MinPOMCP-GO,

		MinPOMCP-GO						MinPOMCP-GO*					
		No constraint		Constraint		Relative Gain (%)		No constraint		Constraint		Relative Gain (%)	
		N_{col}	Cost	N_{col}	Cost	N_{col}	Cost	N_{col}	Cost	N_{col}	Cost	N_{col}	Cost
Cube Baffle	1	2	115.144	0	114.296	100.00	0.74	0	91.912	0	106.072	/	-15.41
	2	0	96.936	0	97.808	/	-0.90	0	93.592	0	95.144	/	-1.66
	3	1	104.360	0	105.688	100.00	-1.27	2	108.848	0	100.720	100.00	7.47
	4	1	102.648	0	98.384	100.00	4.19	0	94.824	0	99.368	/	-4.79
Wall Baffle	1	21	243.848	6	162.936	71.43	33.18	12	179.696	0	116.664	100.00	35.08
	2	14	191.600	3	141.616	78.57	26.09	9	152.024	0	116.720	100.00	23.22
	3	0	85.336	0	95.632	/	-12.07	0	84.816	0	95.768	/	-12.91
	4	3	110.976	2	102.616	33.33	7.53	1	95.216	0	87.280	100.00	8.33
San Diego	1	37	387.776	36	370.904	2.70	4.35	40	385.800	35	355.352	12.50	7.89
	2	39	381.368	31	347.800	20.51	8.80	27	305.408	23	278.600	14.81	8.78
	3	34	355.872	18	249.392	47.06	29.92	32	334.264	8	180.576	75.00	45.98
	4	27	305.496	9	189.824	66.67	37.86	28	311.352	11	199.136	60.71	36.04

Table 1: Comparison of the performance metrics obtained by imposing the best constraint with the ones without constraint. The relative gains are computed as relative changes, taking the performance metric value obtained without constraint as reference. The considerably performance gains are presented in bold.

imposing the best constraint that it returns improves clearly the planning performance even when using the online equivalent, MinPOMCP-GO*.

Conclusion

In this paper, we have proposed a learning-based state abstraction approach to address a partially observable problem of UAV autonomous navigation, where the GNSS availability may have a dramatic impact on the UAV path. We have then implemented a process to learn the best path constraint, *i.e.* the best corridor in which the UAV must navigate, from a set of GNSS availability probability maps. We have evaluated this approach on different environments, including a realistic urban one. The presented results have shown that first, imposing these learnt path constraints based on GNSS availability can indeed improve the quality of the online computed paths, especially when uncertainty is high, and second, it has good performances on problems where only the state space is abstracted, and in situations where the constraint is learnt using one algorithm, and then used online with another algorithm.

Future works will generalize this approach by not only considering the GNSS availability map as feature, but also the initial and goal positions. To do so, we will avoid to evaluate all the possible constraints by only considering the most suitable candidate constraints, in order not to generate a huge number of training data. For example, in our navigation problem, only three constraints may be considered for each feature vector: the one corresponding to the shortest path, the one maximizing GNSS availability probability, and the one weighting the both of them.

References

Abel, D.; Hershkowitz, D. E.; and Littman, M. L. 2016. Near Optimal Behavior via Approximate State Abstraction. In *International Conference on International Conference on Machine Learning (ICML)*. New York City, NY, USA.

Anand, A.; Grover, A.; Mausam, M.; and Singla, P. 2015. ASAP-UCT: Abstraction of State-Action Pairs in UCT. In

International Joint Conference on Artificial Intelligence (IJ-CAI). Buenos Aires, Argentina.

Anand, A.; Noothigattu, R.; Mausam; and Singla, P. 2016. OGA-UCT: On-the-Go Abstractions in UCT. In *International Conference on Automated Planning and Scheduling (ICAPS)*. London, UK.

Bakker, B.; Zivkovic, Z.; and Kröse, B. 2005. Hierarchical dynamic programming for robot path planning. In *International Conference on Intelligent Robots and Systems (IROS)*. Hamburg, Germany.

Carmo, A. R.; Delamer, J.-A.; Watanabe, Y.; Ventura, R.; and Ponzoni Carvalho Chanel, C. 2020. Entropy-based adaptive exploit-explore coefficient for Monte-Carlo path planning. In *International Conference on Prestigious Applications of Intelligent Systems (PAIS)*. (Digital ECAI).

Chitnis, R.; Silver, T.; Kim, B.; Kaelbling, L.; and Lozano-Perez, T. 2021. CAMPs: Learning Context-Specific Abstractions for Efficient Planning in Factored MDPs. In *Conference on Robot Learning*. London, UK.

Delamer, J.-A.; Watanabe, Y.; and Ponzoni Carvalho Chanel, C. 2021. Safe path planning for UAV urban operation under GNSS signal occlusion risk. *Robotics and Autonomous Systems*, 142: 103800.

Dijkstra, E. W. 1959. A Note on Two Problems in Connection with Graphs. *Numerische Mathematik*, 1: 269–271.

Gopalan, N.; desJardins, M.; Littman, M. L.; MacGlashan, J.; Squire, S.; Tellex, S.; Winder, J.; and Wong, L. L. S. 2017. Planning with Abstract Markov Decision Processes. In *International Conference on Automated Planning and Scheduling (ICAPS)*. Pittsburgh, PA, USA.

Hart, P. E.; Nilsson, N. J.; and Raphael, B. 1968. A Formal Basis for the Heuristic Determination of Minimum Cost Paths. *IEEE Transactions on Systems Science and Cybernetics*, 4(2): 100–107.

Hostetler, J.; Fern, A.; and Dietterich, T. 2014. State Aggregation in Monte Carlo Tree Search. In *AAAI Conference on Artificial Intelligence (AAAI)*. Québec City, QC, Canada.

- Jiang, N.; Singh, S.; and Lewis, R. 2014. Improving UCT Planning via Approximate Homomorphisms. In *International Conference on Autonomous Agents and Multi-Agent Systems (AAMAS)*. Paris, France.
- Kaelbling, L. P.; Littman, M. L.; and Cassandra, A. R. 1998. Planning and acting in partially observable stochastic domains. *Artificial Intelligence*, 101: 99–134.
- Keller, T.; and Helmert, M. 2013. Trial-Based Heuristic Tree Search for Finite Horizon MDPs. In *International Conference on Automated Planning and Scheduling (ICAPS)*. Rome, Italy.
- Kleijer, F.; Odijk, D.; and Verbree, E. 2009. Prediction of GNSS Availability and Accuracy in Urban Environments Case Study Schiphol Airport. In *Location Based Services and TeleCartography II. Lecture Notes in Geoinformation and Cartography*. Springer, Berlin, Heidelberg.
- Kocsis, L.; and Szepesvári, C. 2006. Bandit Based Monte-Carlo Planning. In *European Conference on Machine Learning (ECML)*. Berlin, Germany.
- Lee, Y.; Cai, P.; and Hsu, D. 2021. MAGIC: Learning Macro-Actions for Online POMDP Planning. In *Robotics: Science & Systems (RSS)*. (Held Virtually).
- Li, L.; Walsh, T. J.; and Littman, M. L. 2006. Towards a Unified Theory of State Abstraction for MDPs. In *International Symposium on Artificial Intelligence and Mathematics (ISAIA)*. Fort Lauderdale, FL, USA.
- Mettler, B.; Kong, Z.; Goerzen, C.; and Whalley, M. 2010. Benchmarking of obstacle field navigation algorithms for autonomous helicopters. In *Forum of the American Helicopter Society (AHS)*. Phoenix, AZ, USA.
- Ong, S. C. W.; Png, S. W.; Hsu, D.; and Lee, W. S. 2010. Planning under Uncertainty for Robotic Tasks with Mixed Observability. *The International Journal of Robotics Research*, 29(8): 1053–1068.
- Pineau, J.; Gordon, G.; and Thrun, S. 2006. Anytime Point-Based Approximations for Large POMDPs. *Journal of Artificial Intelligence Research (JAIR)*, 27: 335–380.
- Silver, D.; and Veness, J. 2010. Monte-Carlo Planning in Large POMDPs. In *Advances in Neural Information Processing Systems (NeurIPS)*. Vancouver, BC, Canada.